NACA

RESEARCH MEMORANDUM

EXPERIMENTAL INVESTIGATION OF FREE-CONVECTION HEAT TRANSFER IN VERTICAL TUBE AT LARGE GRASHOF NUMBERS

By E. R. G. Eckert and A. J. Diaguila

Lewis Flight Propulsion Laboratory
Cleveland, Ohio

NATIONAL ADVISORY COMMITTEE
FOR AERONAUTICS

WASHINGTON

August 29, 1952

NACA RM E52F30

NATIONAL ADVISORY COMMITTEE FOR AERONAUTICS

RESEARCH MEMORANDUM

EXPERIMENTAL INVESTIGATION OF FREE-CONVECTION HEAT TRANSFER IN VERTICAL TUBE AT LARGE GRASHOF NUMBERS

By E. R. G. Eckert and A. J. Diaguila

SUMMARY

An investigation was conducted to study free-convection heat transfer in a stationary tube closed at the bottom and heated on its vertical walls; the air heated in the tube was continuously replaced by fresh cool air at the top. The tube was designed to provide a gravitational field with Grashof numbers of a magnitude comparable with those generated by the centrifugal field in rotating blade coolant passages (10^8 to 10^{13}). Local heat-transfer coefficients in the turbulent flow range and the temperature field within the fluid were obtained.

Heat-transfer coefficients, converted to dimensionless Nusselt numbers, were correlated as a function of Grashof and Prandtl number parameters. When the heat-transfer coefficients were based on the temperature difference in the horizontal plane under consideration, the Nusselt numbers in the turbulent range investigated averaged 35 percent below the known relations for vertical flat plates.

Several tube-cover configurations that provided different methods of removing and replacing the heated air were investigated. The greatest drop in the temperature of the air in the tube occurred very near the tube wall. This drop indicated that a thin boundary layer existed along the heated wall surface. The temperature of the air in the central axis of the tube increased with distance from the air inlet about 30° F. When the bottom of the tube was closed, the location of warmer, lighter, air below cooler, heavier, air created unstable conditions in the flow. The heat-transfer coefficients determined by use of local temperature differences between the wall and the air in the tube axis as well as the magnitude of the temperature increase along the tube axis were not influenced by the configuration changes.

INTRODUCTION

Interest in the study of free-convection heat transfer recently increased when it was realized that the centrifugal field in rotating components of propulsion systems often creates very strong free-convection

flows. Such flows may, for example, influence considerably the heat transfer in air-cooled rotor blades of gas turbines and explain certain observations in the combustion chambers of rotating ram jets used to propel the rotor blades of helicoptors. Furthermore, it was found that in liquid-cooled turbine rotor blades the free-convection currents alone were sufficient to provide very effective cooling (reference 1). Schmidt (reference 2), who proposed this cooling method, used coolant passages which were drilled into the turbine blade in a spanwise direction in such a manner that the ends of the passages near the blade tip were closed, whereas the inner ends near the blade root were open to a liquid pool. When the blades are heated by the combustion gases and rotated, the heat flow into the cooling fluid which fills the blade passages creates temperature differences within the coolant and in this way sets up rather intense free-convection currents. The Grashof number which characterizes this flow is very high because of the large centrifugal forces, and the flow is consequently in the turbulent range.

Very little experimental information exists on free-convection flow in the Grashof number range above 10^{12} (references 3 and 4). A theory developed in reference 5 to obtain information on the heat-transfer coefficients connected with this type of flow and on the thickness of the heated boundary layer which builds up along the surfaces of the passage starts from the assumption that the flow in a hole of small length-to-diameter ratio is the same as for a vertical flat plate in an infinitely extended fluid. In the development of this theory, the shapes of the temperature and the velocity profiles within the heated boundary layer were assumed. Sufficient experimental data could not be found in the literature to check the assumed profiles.

The experimental investigation described in this report was conducted at the NACA Lewis laboratory in order to check these assumptions indirectly by obtaining a measurement of local heat-transfer coefficients in an arrangement which simulates conditions that exist in the coolant passage of a rotating turbine blade. Difficulties were encountered in checking the velocity and the temperature profiles because of unstable conditions in the test apparatus which will be discussed later.

Detailed measurements in a rotating passage are practically impossible because of the small dimensions involved. Therefore, a stationary apparatus, in which the centrifugal field which generates the free-convection flow in the rotating-blade coolant passage is replaced by the gravitational field, was designed, fabricated, and tested. Conditions for heat transfer should be comparable in both cases as long as the influence of Coriolis forces is neglected (reference 5) and when the Prandtl number for the fluid, as well as the Grashof number, is the same for the rotating and stationary conditions.

This investigation was conducted at a Prandtl number of approximately 0.7 and in a Grashof number range from 10^8 to 10^{13}.

APPARATUS

Basic considerations. - Experiments undertaken to study free-convection flow in a liquid-cooled turbine should be made in the same Grashof number range as, and with Prandtl numbers similar to, those of the cooling fluids used in the application (especially water and MIL-F-5624A, JP-3 fuel).

With regard to the Prandtl numbers, the following fact must be considered. Usually the results of experiments on free-convection flow are plotted as Nusselt number against the product of Grashof and Prandtl numbers with the assumption that Nusselt number depends only on the product of both parameters. Recent experiments and calculations (references 4, 6, 7, and 8) showed that this relation does not hold for a large Prandtl number range. Therefore, the Prandtl number of the test fluid should approximate the Prandtl number of the fluid to be used in the application.

The Grashof numbers which characterize the free-convection flow in a liquid-cooled turbine are very large because of the large centrifugal forces. They were found to extend from 10^{12} to 10^{14} (reference 1). Special provisions are necessary to obtain such Grashof numbers in a stationary apparatus since the gravitational force is much smaller. The Grashof number for free-convection flow under the influence of the gravitational force g is

$$Gr = \frac{l^3 \beta g (t_w - t_a)}{\nu^2} \tag{1}$$

(Symbols are defined in the appendix.)

A high Grashof number can be obtained in an experimental apparatus by use of a fluid with a large β/ν^2 ratio, by providing an apparatus with sufficiently large characteristic dimension l, or by a large temperature difference. The Prandtl numbers Pr, the kinematic viscosities ν, the thermal expansion coefficients β, and the β/ν^2 ratios presented in table I for a number of liquids and gases are based on properties listed in reference 7 and other sources. Mercury has the largest β/ν^2 ratio shown, but the use of this liquid in an apparatus with large dimensions is not convenient. In addition, mercury has a Prandtl number which is very low as compared with the Prandtl number of water or fuel which are usually considered for turbine liquid-cooling applications. Water has a β/ν^2 ratio which increases with temperature. However, the

temperatures in an experimental setup would have to be kept well below 212° F to avoid evaporation when the apparatus is not pressurized. Ethylene glycol, oil, and similar liquids have low β/ν^2 ratios because of their high viscosity, and are not well suited for the contemplated experiments. Very large values of β/ν^2 can be obtained when liquids are near their critical state. Values of β/ν^2 for water and water vapor at a pressure of 200 atmospheres is plotted against temperature in figure 1. Operation near the critical state, however, has the disadvantage that the property values change very rapidly.

In general, gases have lower values of the β/ν^2 ratio than liquids; however, the kinematic viscosity, which is inversely proportional to the density, can be decreased and β/ν^2 increased for gases by an increase in pressure. Air at a pressure of 125 pounds per square inch absolute, for instance, has a value comparable to that of water. In addition, the Prandtl number of air is in the same range as the Prandtl number of MIL-F-5624A (JP-3) fuel and water at temperatures encountered in turbine liquid cooling.

From the previous considerations and for convenience, it was decided to use pressurized air in the apparatus. This apparatus consisted essentially of a vertical tube, closed at the bottom; the walls were heated so that heat was transferred to the pressurized air which filled the tube. Some provision had to be made at the top of the tube to replace the heated air, which rose along the tube wall, by fresh cooled air. The dimensions of the apparatus had to be quite large in order to attain the desired Grashof number range. Steam was used to heat the tube walls in order to insure a uniform temperature of the walls, and to make the determination of the local heat flows convenient. The heat flow was based on the amount of condensate collected in small chambers.

Tube arrangement. - The apparatus which was developed from these basic considerations is shown in figure 2(a). Various component parts are designated by letter on the figure to simplify references in the text. The over-all dimensions of the tube are: height, $13\frac{1}{2}$ feet; diameter, 24 inches; and wall thickness, 3/8 inch. The tube was fabricated from mild steel and coated with zinc on the inside and outside surfaces. The inside surface was ground smooth after the coating was applied. The height of the remaining roughness of the wall along the axial length adjacent to the steam chambers was measured and found not to exceed ±0.007 inch. This variation was assumed to be permissible on the basis of friction data obtained with forced flow through a tube with rough surfaces.

Air at approximately 80° F and 23 to 125 pounds per square inch absolute pressure was introduced at the top cover A. Monel-wire screening B, which produced a large pressure drop, was installed at the air inlet to insure uniform downward flow of the air. The wire screen consisted of two layers of 30X28 mesh (0.013-inch-diameter wire) and two layers of 50X40 mesh (0.0059-inch-diameter wire) stacked at 45° to each other. The desired pressure in the tube was obtained with throttle valves in the inlet and outlet lines (C and D, respectively). An orifice in the air-supply line was used to measure the air flow to the tube.

The surface of the tube was heated with low-pressure steam superheated by throttling to 2° or 3° F above the saturation temperature; the pressure ranged from 1 to 3 inches of mercury above atmospheric pressure. Four openings E along the length of the insulated steam jacket surrounding the tube were used to distribute the steam uniformly throughout the jacket F. A steam trap on the main condensate line and a throttle valve on the steam supply line were used to obtain the desired steam pressure.

Sixteen condensate chambers G, $7\frac{1}{2}$ inches wide, were arranged along the length of the heated section of the tube; therefore, only part of the circumference of the tube was covered. The chambers varied in length from 6 inches at the top of the tube to $8\frac{1}{2}$ inches at the bottom and trapped only the condensate which developed on the section of the tube wall enclosed by these chambers. From each chamber, 1/2-inch-diameter lines, shown in figure 2(b), carried the condensate through the steam jacket to the condensate measuring apparatus. The exposed portion of these lines (H in fig. 2(a)) was heavily insulated to reduce heat losses.

After the desired information was obtained with the arrangement shown in figure 2(a), the method in which the air was introduced to the tube was altered in order to study its effect on heat transfer. The top cover A was replaced by the redesigned cover J. This cover admitted air over the entire tube cross section, whereas in the first cover, a ring section was provided around the wall to separate the rising, heated air stream from the incoming fresh, cool air. The new cover contained screening B consisting of a 1/8-inch-thick Fiberglas mat between two 1/4-inch mesh (23-gage wire) galvanized screens to insure uniform air velocities. The bottom plate K of the first configuration was replaced by a cover identical to cover J to permit the introduction or exhaust of air at the bottom of the tube; this cover also made possible a study of superimposed free and forced convection.

In a third configuration, the top cover or both top and bottom covers A and K were removed so that room air could circulate into or through the tube. In one test a screen identical to the one in cover J was placed across the bottom opening to reduce the air flow.

Condensate measuring apparatus. - The condensate from the condensate chambers was measured on a burette board, L in figure 2(a). Each chamber G was connected to a burette M graduated in tenths of a milliliter. A spherical condensate collector N, $1\frac{3}{4}$ inches in diameter, and a petcock O arrangement at the top of the burette were necessary for the following reason.

Direct connections between the burettes and the lines from the condensate chamber H would permit steam to fill the portions of the burettes not filled with condensate and thus provide an exposed area for steam condensation which would vary with the amount of condensate in the burettes.

The burettes were insulated by two layers of air between two Plexiglas windows at the front and an insulating board at the rear. Nevertheless, the condensation caused by the heat losses from the burettes proved inconvenient in the first runs made with direct connections between burettes and condensate lines. The spherical container N was emptied into the burette as soon as the condensate level had risen to about 1/4 inch above the level indicated in figure 2(a); this provided a relatively large volume of condensate and a small variation in exposed surface area on which steam would condense. The tube, inserted in the container N to slightly below the center, provided a minimum condensate level in the sphere which could be conveniently reproduced. The time required to obtain this amount of condensate ranged from 15 to 30 minutes depending upon the operating condition and the position of the condensate chambers.

Instrumentation. - Five iron-constantan thermocouples P, spaced as shown in figure 2(a), were used to measure the wall temperatures. These thermocouples were embedded in holes drilled from the outside into the tube wall to a depth of 1/4 inch. The thermocouple ends were welded into a small copper cylinder which fitted the holes closely. Thermocouple lead wires were attached to the outside wall of the heated tube and brought out of the steam jacket through the bottom flange. Fiberglas insulation and plastic coating protected the thermocouple wires from the steam. Two thermocouples Q were also used on the tube wall below the heated section to determine tube-wall temperatures. Steam temperatures were measured by four iron-constantan thermocouples R spaced along the length of the steam jacket. Each thermocouple was so arranged in a 1/8-inch-diameter tube that the junction was formed by welding the ends into a cap closing the tube. The thermocouple junctions were located midway between the tube wall and steam-jacket wall.

Originally, the temperatures of the air inside the tube were to be measured with a resistance thermometer (fig. 3(a)). A bridge, a galvanometer, and a battery circuit, which measure the change of resistance with temperatures of a 0.0004-inch-diameter nickel wire, are used with this type of thermometer. Fluctuations of the air temperature, however, made reading with this instrument very difficult. It was therefore used only in certain runs to measure the air temperatures along the center line of the tube.

In most cases the air temperatures inside the tube were measured with the thermocouple probes shown in figure 3(b). The probe locations and identification numbers along the length of the tube are shown by S in figure 2(a). The probes traversed from the center of the tube to the tube wall adjacent to the condensate chambers by means of a motor driving arrangement on the probe mounting. With this arrangement it was possible to obtain temperature readings of the heated air in five planes at any desired radius. Air temperatures were also measured with iron-constantan thermocouples in the inlet and outlet lines.

The air pressure in the tube was measured with calibrated Bourdon type gages through pressure taps at two locations, one near the top and one near the bottom of the tube wall.

Accuracy of Measurements

Calculation of the heat-transfer coefficients on the inside wall of the tube is based on the air temperature along the axis of the tube and on the temperature of the heated-wall surface. Since the temperature near the center of the wall, where the thermocouples are located, is higher than at the inside wall surface, a calculation of the temperature drop due to the heat conduction through the wall was made; a temperature difference of approximately 1° F was indicated. The accuracy of the potentiometer, the calibration accuracy, and the reading accuracy together added up to an error in the wall-temperature measurement of $\pm 2.0^{\circ}$ F. The calculated temperature difference between midwall temperature and surface temperatures was within this range and was therefore disregarded. The difference between the temperatures indicated by the thermocouples in the steam chest and in the wall was between 0.5° and 1° F. Steam temperatures and air temperatures were estimated to be accurate within $\pm 1.5^{\circ}$ F. Repeated readings of the temperature of the heated air at a specified location, however, were only within $\pm 3^{\circ}$ to $\pm 5^{\circ}$ F depending on location of the thermocouples. These fluctuations of the air temperature will be discussed later.

The mercury U-tube measurements of the steam pressure were accurate within ±0.05 pounds per square inch. The saturation temperature determined from this pressure agrees within 1° F with the steam temperature measured by the thermocouples. Air pressures were measured with Bourdon type gages. The difference between the readings of the gages was small and the average of both was used to determine the air density. The accuracy of these measurements determined by calibration was found to be 2 percent below 30 pounds per square inch absolute and 1 percent above this value. The condensate was collected during the runs and measured volumetrically. Duration of the runs was determined with a stop watch. The measurements of the rate of condensation for the complete run could be reproduced within ±2.0 percent. The flow orifice for the supply air was calibrated and estimated to be accurate within 1 percent.

CALCULATION OF LOCAL HEAT-TRANSFER COEFFICIENTS

Equation Defining Heat-Transfer Coefficient

The local film heat-transfer coefficients inside the tube at various locations along its length were determined from the following equation:

$$H = \frac{Q_c}{A(t_w - t_a)} \tag{2}$$

In this equation the area A considered for heat transfer was that section of the inside surface of the tube which was enclosed by the individual condensate chamber. Included in this value is one-half the thickness of the walls of the condensate chambers attached to the tube wall. The total thickness of the condensate-chamber wall is 0.05 inch. The temperature of the air t_a in equation (2) was obtained along the tube axis directly opposite the center of the condensate chamber. Only five air temperature measurements were made along the axis; therefore, the air temperatures opposite the centers of the individual condensate chambers were determined from a curve faired through these measured temperatures. The temperature measured in the center of the tube wall was used in equation (2) as the wall temperature t_w. This temperature was constant along the tube.

Evaluation of Convective Heat Flow and Heat Loss

Determination of convective heat flow Q_c. - The total heat flow Q was determined by measurement of the condensate collected in the individual burettes. This condensate, however, consisted not only of the amount collected in the individual condensate chambers (G in fig. 2(a))

but also of the amounts formed by the heat flow to the surrounding atmosphere from the part of the condensate lines outside the steam jacket (H in fig. 2(a)) and the spherical condensate collectors (N in fig. 2(a)). In addition, heat is transferred from the interior tube surface not only to the air by convection but also to the cooler top and bottom sections by radiation. Correspondingly the convective heat flow per unit time Q_c may be determined from the equation

$$Q_c = Q - Q_A - Q_R \tag{3}$$

where

$$Q = wh \tag{4}$$

The heat flow to the surrounding atmosphere from the condensate lines and in the spherical collectors is denoted by Q_A and the radiative heat flow by Q_R in equation (3). In equation (4), the condensate weight flow per unit time is w, the total measured rate for the individual burette corresponding to the condensate chamber (or location along the tube surface) under consideration. The term h is the heat of vaporization per pound of water at saturation pressure, that is, the measured pressure in the steam jacket. The small degree of superheating was neglected. The heat flow Q obtained by use of equation (4) is therefore the total heat released by condensation of the weight w.

Determination of heat loss $Q_A + Q_R$. - In order to determine the convective heat flow Q_c it is necessary to subtract from the total heat flow Q the heat lost to the atmosphere Q_A from the exposed condensate lines and collectors, and the heat radiation Q_R. Both quantities were determined in heat-loss runs. If the tube could be evacuated, heat would be removed from the interior tube wall only by radiation towards the cooler top and bottom sections. The condensate collected in such a run was the result of this radiative heat flow Q_R and the heat losses in the condensate lines and spherical collectors Q_A.

Actually, the laboratory facilities which were connected to this apparatus did not provide complete evacuation of the tube. Therefore, a small convective heat transfer still took place in the interior of the tube, and equation (3) holds for such heat-loss runs as well as for heat-transfer runs. The convective heat flow is, however, much smaller because of the lower density of the air and because the heated air inside the tube is not replaced in these runs but is heated to a temperature near that of the wall. This convective heat flow encountered in heat-loss runs may be indicated by Q_c' and the amount of condensate collected in such a run by w'. Then the equation (3) becomes

$$Q_c' = w'h - Q_A - Q_R \tag{5}$$

When the room conditions are the same, the heat lost from the condensate lines and the spherical collectors Q_A and from radiative flow Q_R is the same as in the actual heat-transfer runs; this heat loss can be computed by use of equation (5).

If equations (3) to (5) are combined,

$$Q_c = wh - w'h + Q_c' \tag{6}$$

In this equation w is the amount of condensate collected during a heat-transfer run, w' is the amount collected during a heat-loss run, and Q_c' is the convective heat transfer in a heat-loss run. The value of Q_c' is small compared with the other terms in equation (6) under the test conditions set up in the heat-loss runs and can be determined by an approximate calculation. The equation for the average Nusselt number in free-convection laminar flow (reference 4) on a vertical plate is

$$\overline{Nu} = 0.555 \, (Gr \, Pr)^{1/4} \tag{7}$$

The local Nusselt number which follows was obtained from this relation by multiplying by the factor 3/4 (reference 7, p. 162):

$$Nu = 0.416 \, (Gr \, Pr)^{1/4} \tag{8}$$

The laminar equation was used to obtain the convective heat-transfer coefficient for the conditions existing in the tube during the heat-loss runs because the low density of the air in the tube and the small temperature difference lowered the Grashof number for these runs below the critical value. The convective heat flow Q_c' was calculated by use of equation (2) and the temperatures t_w and t_a which were measured during these runs. All data were then available to calculate the convective heat flow Q_c in equation (6). The convective heat flow Q_c' encountered during the heat-loss runs amounted to 2 to 4 percent of the convective heat flow Q_c in the heat-transfer runs.

Alternate method of determining heat loss. - A calculation was also made to obtain an estimate of the heat flow by radiation Q_R from the heated walls to the unheated top and bottom sections of the tube. In this calculation, the temperature of the tube surface was assumed to be 212° F and that of the bottom circular surface 90° F. This temperature range is representative of the severest conditions. The emissivity of the galvanized iron surface was taken as 0.20. For the heat-transfer runs, the heat

exchange by radiation between the center of the wall section enclosed by the lowest condensate chamber and the bottom plate was calculated on these assumptions to be approximately 0.75 percent of the convective heat flow Q_c. At other locations along the tube wall, the radiative heat transfer was still smaller; therefore, the heat transfer by radiation could be neglected.

The heat loss Q_A in the condensate lines and the spherical collectors can be determined by arranging traps at the location where the condensate lines leave the steam jacket. These traps were so designed that no condensate coming from the condensate chambers could flow into the spherical collectors. These collectors then collected only condensate formed on their surfaces and that which formed within the condensate lines outside the steam jacket. From the condensate measured in the burettes by this method, the heat loss Q_A could be found. The traps were arranged only on a selected number of condensate lines in order to check the heat losses obtained by the first method described. Convective heat flows Q_c determined in this manner agreed with the values obtained by the first method within 3 percent.

EXPERIMENTAL PROCEDURE

Heat-loss runs. - The purpose of the heat-loss runs was to determine the heat loss Q_A (in the condensate lines and the spherical collectors) and the radiated heat Q_R as described in the section Determination of heat loss, and also to obtain the information necessary for calculating the convective heat flow Q_c'. In the heat-loss runs, the tube was partially evacuated by reducing the air pressure to 7 inches of mercury absolute, the minimum permitted by the available laboratory altitude-exhaust facilities. Before the data were recorded, the tube was heated by the low-pressure steam for approximately 2 hours. This length of time was required for the tube-wall temperatures of the heated and unheated sections and the temperature of the air in the tube to reach equilibrium. After equilibrium was obtained, the quantity of condensate in the burettes was recorded at 20-minute intervals and an average of at least five readings was obtained. The heat-loss runs were repeated at various intervals throughout the investigation. Air temperatures in the tube and tube-wall temperatures in a heat-loss run are presented in figure 4. From these temperatures and the Nusselt numbers given by equation (8), it was possible to calculate the heat transfer Q_c' in the tube during the heat-loss runs. The heat losses Q_A and Q_R determined in this manner increased from 20 percent of the total heat-flow rate Q at the high-pressure runs to 45 percent for the low-pressure runs.

Heat-transfer runs. - Heat-transfer runs were made for a series of air pressures inside the tube between atmospheric and maximum air-supply

pressure (125 lb/sq in. abs) in order to obtain the desired range of Grashof numbers. Runs were also made with different amounts of air flowing through the upper part of the tube. The purpose of this variation was to detect the influence of air-flow rate on the air-temperature distribution in the tube and on the heat transfer. For each run, the tube was preheated for a period of approximately 2 hours and data were then taken at 20-minute intervals over a period of 2 to 3 hours. Throughout each run, conditions were carefully kept constant. The measurements produced all necessary data for calculating local heat-transfer coefficients. In addition, the temperature field of the air inside the tube was investigated by measurement of the temperature profiles along the cylinder radii in the planes indicated in figure 2(a) by the probes S.

In the course of the investigation, the method by which the heated air in the tube was replaced was changed in order to study its effect on the temperature field and the heat transfer. For this purpose, the top and bottom covers were changed as described in the APPARATUS section.

RESULTS AND DISCUSSION

Temperature field. - The air-temperature distribution within the tube is shown in figures 5 to 9. The results of measurements on the first cover configuration, shown in figure 2(a), are presented in figures 5 and 6. The data obtained with the second cover configuration are presented in figures 7 and 8. The air-temperature measurements of other configurations studied are shown in figure 9.

Temperature profiles along tube radii measured at different tube heights are presented in figures 5 and 7; figures 6, 8, and 9 show temperatures measured along the tube axis. Included in these figures are inlet air and wall temperatures. Temperature profiles measured with probe 5 are not shown because the temperature fluctuations in this plane were too large to permit reproducible measurements.

When this investigation was started, it was assumed that the air which is heated along the cylindrical surface of the tube would rise within a thin layer along this surface and would be removed through outlets D (fig. 2(a)), and that the air temperature in the central core of the tube would be quite uniform. Figure 5 shows that the essential temperature drop actually occurs very near to the tube wall, however, figure 6 indicates that an appreciable increase in temperature with distance from the air inlet occurs in the central core; the amount of increase is approximately 30° F. Inspection of the various curves reveals that the differences between the individual curves in figures 6(a) and 6(b) cannot be connected with the pressure of the air in the tube nor with the amount of air passing through the top portion of the tube. Such a temperature distribution (with warmer, and therefore lighter, air layers

below cooler, and therefore heavier, ones) creates a very unstable state which can exist only in the presence of dynamic and viscous forces connected with flow. It is therefore understandable that the flow in the central core is fluctuating and turbulent. This condition is also indicated by the temperature fluctuations encountered especially in the upper portion of the tube. These fluctuations are probably responsible for the heat transferred from the hot boundary layers along the wall into the central portion of the tube.

A question then arises as to what degree the temperature distribution in the core of the air is influenced by the specific method used in removing the warm air stream along the wall from the top of the tube and to replace it by fresh cool air. One arrangement investigated involved replacing the top cover A (fig. 2(a)) by cover J. The bottom plate K was exchanged for an identical cover J; however, no air was admitted or removed through the bottom cover; thus, its action was not different from that of plate K. Air was admitted through the top cover J and removed through the exhaust lines D. The results of the air temperature measurements are presented in figures 7 and 8. Again, a thin, heated boundary layer is indicated near the tube wall. Also, a temperature increase with distance from the air inlet along the tube axis is present and the amount of the increase throughout the tube is approximately 30° F. The various curves, which are closer together, indicate more stable conditions than for the first configuration. The temperature measurements in the central plane (fig. 8) were made with the resistance thermometer, whereas all the other temperature measurements were made with iron-constantan thermocouples.

A more radical change in the air-flow conditions was obtained in the following way. The top cover was removed so that the tube was opened to room air. The hot boundary layer discharged into the room was thus replaced by cool air flowing into the open top of the tube. The temperatures along the tube axis, which are shown in figure 9 (curve A), indicate an increase with distance from the inlet of approximately the same magnitude as before. When part of the air is admitted into the bottom of the tube through screening consisting of a 1/8-inch-thick Fiberglas mat between two 1/4-inch-mesh (23 gage wire) galvanized screens, a temperature increase with distance from the lower inlet occurs in the lower portion of the tube, whereas the temperature field in the upper portion is essentially the same as it was with the previous configuration. Curve B (fig. 9) shows the temperatures for this case. Only when the screen at the bottom was removed and the tube was open at both ends did the temperature along the axis become nearly uniform (fig. 9, curve C). A temperature distribution similar to curve B was obtained in the second cover configuration, when part of the air was admitted through the upper and part through the lower cover (fig. 9, curve D).

The investigation indicates that a temperature variation along the tube axis is consistently associated with the specific configuration which

provides free-convection flow in a tube closed at the bottom and heated along its walls. Such a configuration corresponds to the liquid-cooling arrangement for turbines proposed by Schmidt. The magnitude of the temperature increase is approximately the same regardless of the covor configuration. In addition, the essential difference in the temperature distributions for the individual runs is a general change in the temperature level which may be determined by the degree of mixing of the leaving and incoming air streams.

In figure 10, the ratio of the temperature difference between the wall and the air along the center line of the tube to the same temperature difference near the inlet (probe 5, fig. 2(a)) is plotted against the tube length for the first cover configuration, the second cover configuration and with the top cover removed. It can be observed that no apparent difference in this temperature ratio exists for these configurations. For the Grashof and Prandtl number ranges investigated, the curve faired through the observed points represents the average temperature increase of air in a vertical tube closed at the bottom, heated along the wall, and having a length-to-diameter ratio of 5.

In order to obtain additional information on the air flow in the core of the tube, a scale model one-sixth the actual size was fabricated from pyrex glass with a top cover similar to J shown in figure 2(a). The model was not heated because the object was to obtain only information on how the flow in the tube is affected by the inlet and outlet configuration. The model was filled with smoke and then clear air was introduced at the top. A photograph of this apparatus during the smoke test is shown in figure 11. It may be observed that the smoke is quite dense in the lower third of the tube indicating that very little mixing of the air occurs in this portion of the tube. In the central third of the tube, the smoke is still present but it is less dense indicating a slight degree of mixing. In the upper third of the tube the air is completely clear as a result of considerable mixing with the air supplied at the top. The Reynolds number for the air flow under the conditions shown in figure 11 was lower than in the full-scale test apparatus. Visual observations, however, were made up to Reynolds numbers which almost equaled those in the full-scale apparatus. No appreciable change in flow pattern could be observed for increasing Reynolds number.

Heat-transfer coefficients. - Local heat-transfer coefficients were calculated by use of equation (2). Local coefficients were converted to dimensionless Nusselt numbers; a characteristic length l, which will be discussed later, was used in this conversion. Nusselt numbers are plotted in figures 12(a) to 12(c) against the product of Grashof and Prandtl numbers. This parameter is customarily used in free-convection correlations and it was retained here although, as pointed out in the APPARATUS section, recent investigations indicate that it does not apply for a large Prandtl number range.

The property values of the air were introduced into the dimensionless number at a reference temperature equal to the arithmetic mean between wall temperature and air temperature at the tube axis. The readings on the burette connected with the highest condensate chamber were consistently low. Consequently, the coefficients for the section of the tube adjacent to the highest condensate chamber were omitted in figures 12(a) to 12(c). The range of Grashof numbers extends from 10^8 to 10^{13}, which is higher than the ranges covered in previous investigations. In these figures, curves representing local Nusselt number relations for free-convection flow on a vertical flat plate in the laminar and the turbulent ranges are also included. The line representing heat transfer for laminar flow corresponds to equation (8). The following relation for average Nusselt number is given in reference 5 for free-convection heat transfer under turbulent flow conditions:

$$\overline{Nu} = 0.0210\ (Gr\ Pr)^{2/5}$$

This relation, which is in agreement with relations given in references 3 and 4 for the range of this investigation, shows that for turbulant flow the heat-transfer coefficient is proportional to the 1/5 power of the distance from the lower-plate end and that the local Nusselt number is 1.20 times the average value. Therefore, the relation for the local heat-transfer coefficient is

$$Nu = 0.0252\ (Gr\ Pr)^{2/5}$$

These equations hold for a vertical plate with uniform temperature, but the wall temperature of the tube was constant only where it was surrounded by the steam chest (fig. 2(a)). In the portion below the steam chest, the wall temperature decreased with distance from the air inlet. In order to account for this fact a fictive end of the heated section was established as indicated in figure 13. In this figure, the measured wall temperatures are plotted against distance from the lower end of the steam chest. The air temperature along the tube axis as extrapolated from the measured values is also indicated on the figure. It can be seen that the temperature difference between the wall and the air decreases with distance below the end of the steam chest and reaches a value of zero, 8 inches below the jacket for this particular run. It can be expected that in a first approximation, conditions are similar on a tube with a constant temperature difference which has its lower end at a position such that the two dashed areas in figure 13 are equal. In this way, the expression $\int (t_w - t_a)dA$, which is important for the heat transferred, becomes equal for the real tube and the one with a constant temperature difference. The fictive end of the steam chest was determined in this way. The characteristic length l contained in the Nusselt and Grashof numbers was measured from the fictive end of the steam chest to

the center of the condensate chamber being considered. This length influences Nusselt and Grashof numbers only for the two lower condensate chambers. Figure 12(a) shows the Nusselt and Grashof number calculated for two points with the effective length l measured from the lower end of the steam chest to the centers of the lower two condensate chambers. These points are connected by arrows, with corresponding points calculated by use of the distance from the fictive end of the steam chest for the characteristic length.

Figure 12 indicates that the Nusselt numbers obtained generally correlate satisfactorily as functions of the Grashof number for all arrangements investigated. In the laminar range, the measured values are above the curve for the local laminar Nusselt relation for a vertical flat plate. In the turbulent range, the mean value of the data is displaced below the curve for the local Nusselt relation for a vertical flat plate by approximately 35 percent. The fact that the degree of scatter of the measured values for the second cover configuration (fig. 12(b)) is less than for the first configuration (fig. 12(a)) confirms the conclusion that the flow conditions in the core were more stable for this configuration.

The figures also show that the way in which the heated air is removed and replaced by fresh air does not influence the heat-transfer coefficients when these are determined by use of local differences between wall temperature and air temperature along the tube axis. The experiments indicate that it is possible to obtain an approximate value of the heat-transfer coefficients in tubes closed at the lower end and heated around the surface for a small length-to-diameter ratio (approximately five) from known relations for vertical flat plates. A calculation of the heat transferred requires the knowledge of the air temperature along the tube axis. An approximate value of the temperature increase of the air along the axis can be obtained from the curve in figure 10.

SUMMARY OF RESULTS

The following results were obtained in an investigation of free-convection flow within a stationary tube closed at the bottom, heated around the periphery, and having a length-to-diameter ratio of approximately 5; the heated air was continuously replaced by fresh, cool air at the top. Conditions that exist within the coolant passages of a rotating turbine blade were simulated in the tube.

1. The greatest drop in the temperature of the air in the tube occurred very near to the tube wall. This drop indicated that a thin boundary layer existed along the heated-wall surface.

2. The temperature of the air in the core of the tube increased with distance from the air inlet. Such a temperature distribution creates unstable flow conditions. The magnitude of the temperature increase did not appear to be influenced by the specific air inlet and outlet configurations.

3. The method of removing and replacing the heated air did not influence the heat-transfer coefficients when these were determined by means of local temperature differences between the heated wall and the air along the tube axis.

4. Heat-transfer coefficients, which were converted to dimensionless Nusselt numbers, correlated as functions of the Grashof numbers. The range of Grashof numbers investigated extended from 10^8 to 10^{13}, which is beyond the range previously investigated.

5. In the turbulent range investigated, the mean values of the Nusselt numbers were approximately 35 percent below known relations for vertical flat plates. These relations may be used to obtain approximate heat-transfer coefficients in heated tubes having a length-to-diameter ratio of approximately 5.

Lewis Flight Propulsion Laboratory
National Advisory Committee for Aeronautics
Cleveland, Ohio

APPENDIX - SYMBOLS

The following symbols are used in this report:

A	inside area of section of tube surrounded by condensate chamber, sq ft
c_p	specific heat of fluid at constant pressure, Btu/(lb)($^\circ$F)
Gr	Grashof number, $\frac{l^3\beta g(t_w-t_a)}{\nu^2}$
g	acceleration due to gravity, 32.2 ft/sec^2
H	local heat-transfer coefficient, Btu/($^\circ$F)(sq ft)(sec)
$\overline{H}$	average heat-transfer coefficient, Btu/($^\circ$F)(sq ft)(sec)
h	heat of vaporization of water, Btu/lb
k	thermal conductivity of fluid, Btu/($^\circ$F)(ft)(sec)
l	characteristic length, ft
Nu	local Nusselt number, Hl/k
$\overline{\text{Nu}}$	average Nusselt number, $\overline{H}l/k$
Pr	Prandtl number, $\frac{c_p\mu}{k}$
Q	heat flow, Btu/sec
t	temperature, $^\circ$F
w	condensate weight flow, lb/sec
β	coefficient of thermal expansion of fluid, 1/$^\circ$R
μ	dynamic viscosity of fluid, lb/(sec)(ft)
ρ	density of fluid, lb/cu ft
ν	kinematic viscosity of fluid, μ/ρ, sq ft/sec

Subscripts:

A atmosphere

a air

c convective

R radiation

w wall

Superscript:

' values obtained in heat-loss runs

REFERENCES

1. Diaguila, Anthony J., and Freche, John C.: Blade-to-Coolant Heat-Transfer Results and Operating Data From a Natural-Convection Water-Cooled Single-Stage Turbines. NACA RM E51I17, 1951.

2. Schmidt, E.: The Possibilities of the Gas Turbine for Aircraft Engines. Reps. and Trans. No. 489, GDC 2504T. British M.O.S.

3. McAdams, William H.: Heat Transmission. McGraw-Hill Book Co., Inc. 2nd ed., 1942, pp. 237-251.

4. Jakob, Max: Heat Transfer. Vol. I. John Wiley and Sons. Inc., 1949, pp. 522-542.

5. Eckert, E. R. G., and Jackson, Thomas W.: Analytical Investigation of Flow and Heat Transfer in Coolant Passages of Free-Convection Liquid-Cooled Turbines. NACA RM E50D25, 1950.

6. Hyman, Seymour C., Bonilla, Charles F., and Ehrlich, Stanley W.: Natural Convection Transfer Processes. I - Heat Transfer to Liquid Metals and Non-Metals at Horizontal Cylinders. Preprints of papers for Heat Transfer Symposium, (Atlantic City, N. J.), Am. Inst. Chem. Eng., Dec. 5, 1951.

7. Eckert, E. R. G.: Introduction to the Transfer of Heat and Mass. McGraw-Hill Book Co., Inc., 1950, pp. 158-171.

8. Ostrach, Simon: An Analysis of Laminar Free-Convection Flow and Heat Transfer About a Flat Plate Parallel to the Direction of Generating Body Force. NACA TN 2635, 1952.

TABLE I - PROPERTY VALUES CONSIDERED IN FREE-CONVECTION STUDIES OF VARIOUS FLUIDS

	Prandtl number Pr	Kinematic viscosity ν (sq ft/sec)	β $\frac{1}{^{\circ}R}$	β/ν^2 $\left(\frac{sec^2}{(^{\circ}R)(ft)^4}\right)$
Liquids at temperature of 68° F (saturated state)[a].				
Mercury	0.0249	0.123×10^{-5}	[b]0.101×10^{-3}	667×10^{5}
MIL-F-5624A (JP-3) fuel	12.3	1.04	.725	67.1
Water	7.02	1.08	.10	8.5
Water (212° F)	1.74	.316	.35	351
Ethylene glycol	204	20.6	.36	.0845
Engine oil (unused)	10,400	970	.39	.0000415
Gases at temperature of 122° F and pressure of 14.22 pounds per square inch[a].				
Freon-12	0.84	3.17×10^{-5}	1.72×10^{-3}	17.1×10^{5}
Carbon dioxide	.79	10.86	1.72	1.46
Ammonia	.91	18.9	1.72	0.483
Air	.70	19.89	1.72	0.434
Arr (125 lb/sq in.)	.70	2.26	1.72	33.65
Hydrogen (212° F)	.65	174.2	1.49	.00492

[a]Except where noted.
[b]This value in error in reference 7.

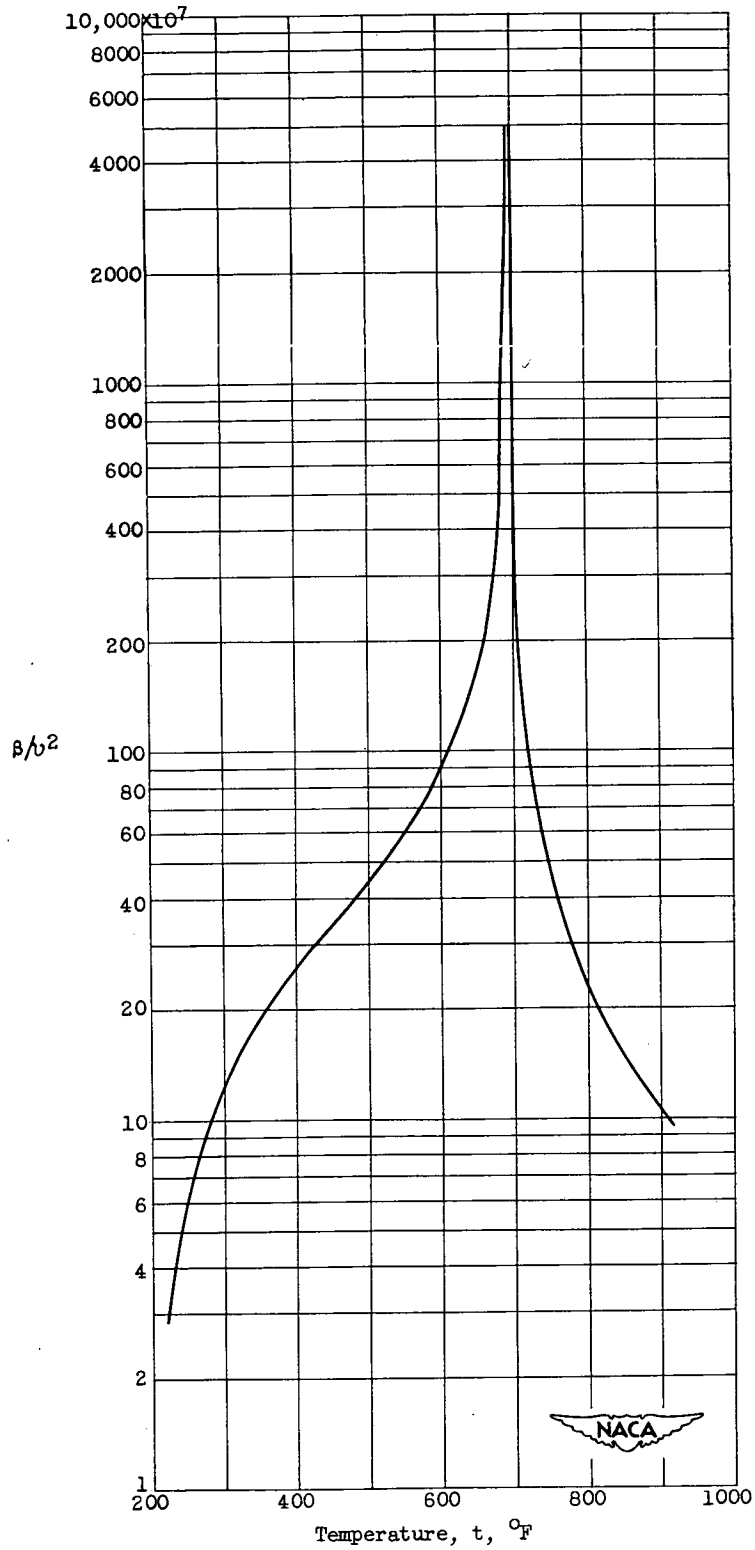

Figure 1. - Values of β/v^2 for water and water vapor near critical state (200 atm).

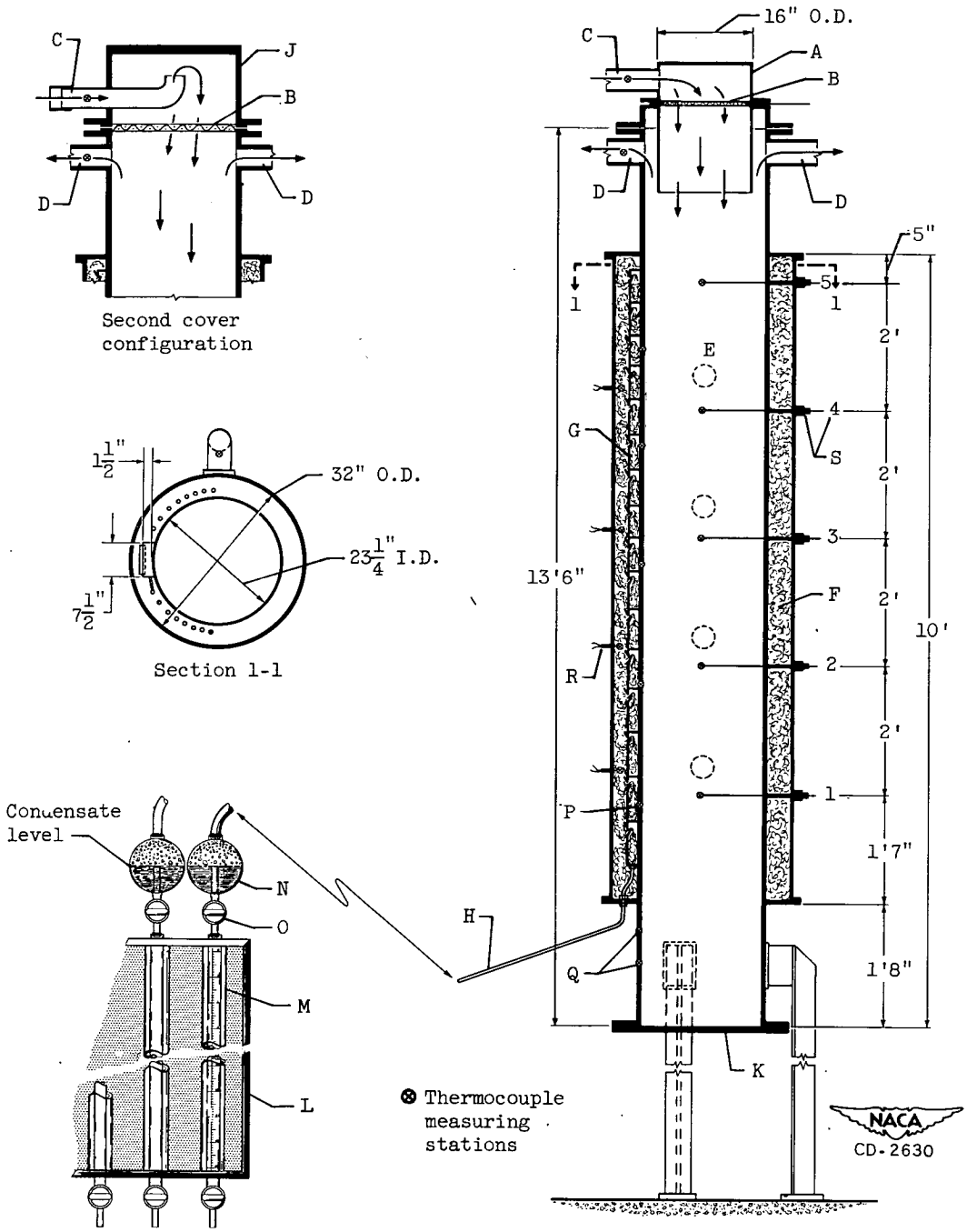

A Top cover of configuration 1
B Screening
C Inlet
D Outlet
E Openings in steam jacket
F Steam jacket
G Condensate chamber
H Exposed portion of condensate line
J Top cover for configuration 2
K Bottom plate
L Burette board
M Burette
N Spherical condensate collector
O Petcock
P Heated wall thermocouple
Q Unheated wall thermocouple
R Steam thermocouple
S Thermocouple probes

(a) Apparatus.

Figure 2. - Free-convection tube.

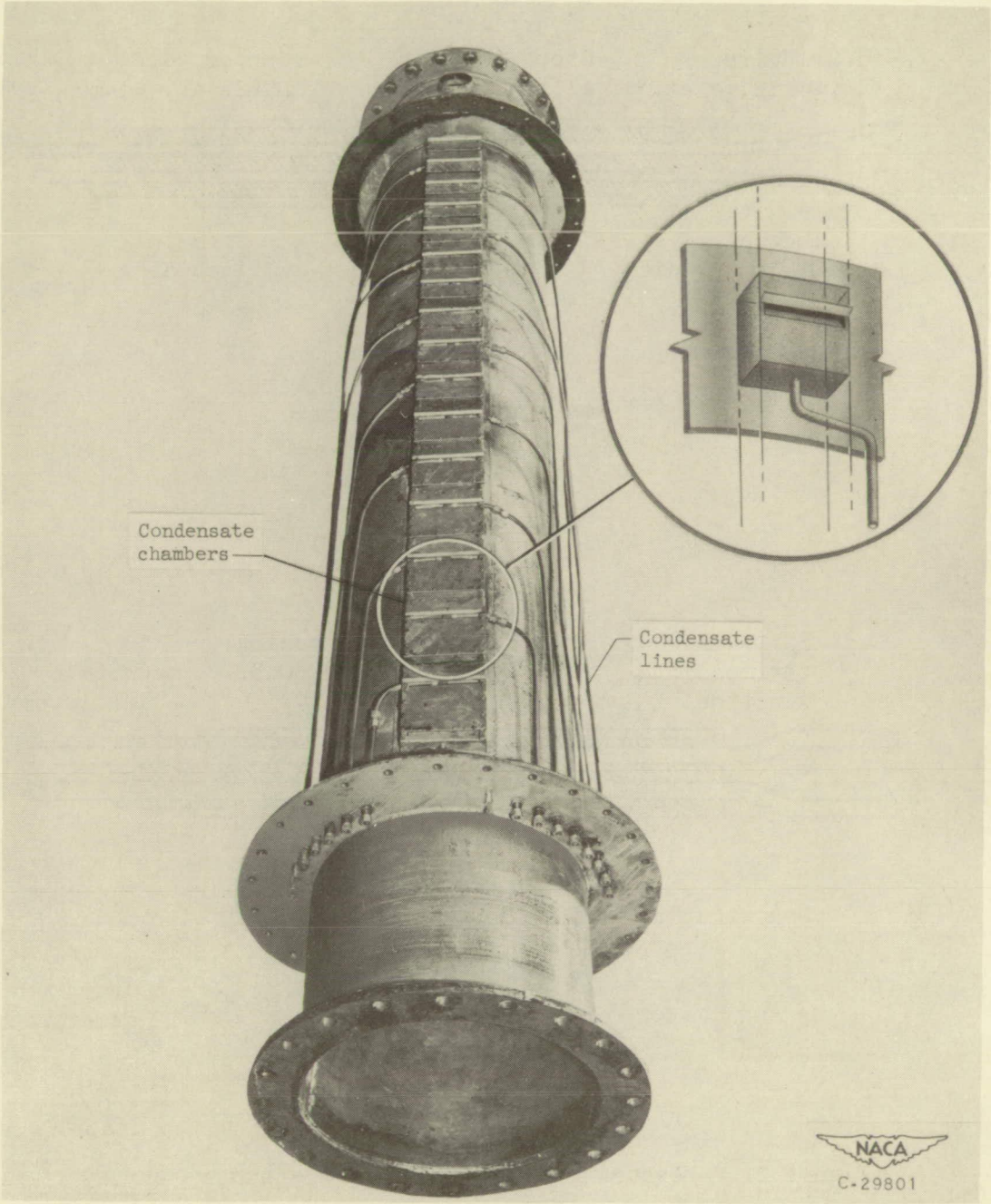

(b) Tube with steam jacket removed showing condensate chambers and condensate flow lines.

Figure 2. - Concluded. Free-convection tube.

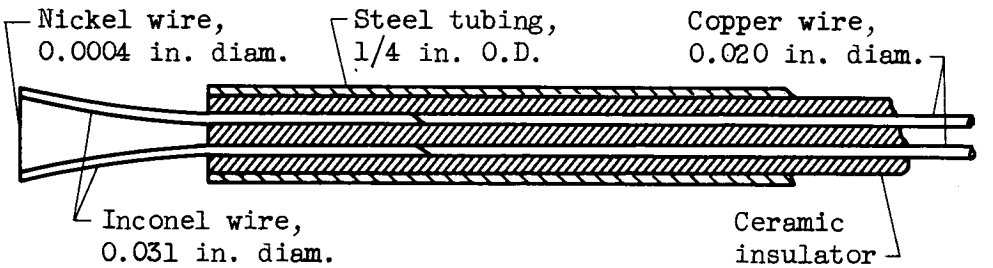

(a) Resistance thermometer.

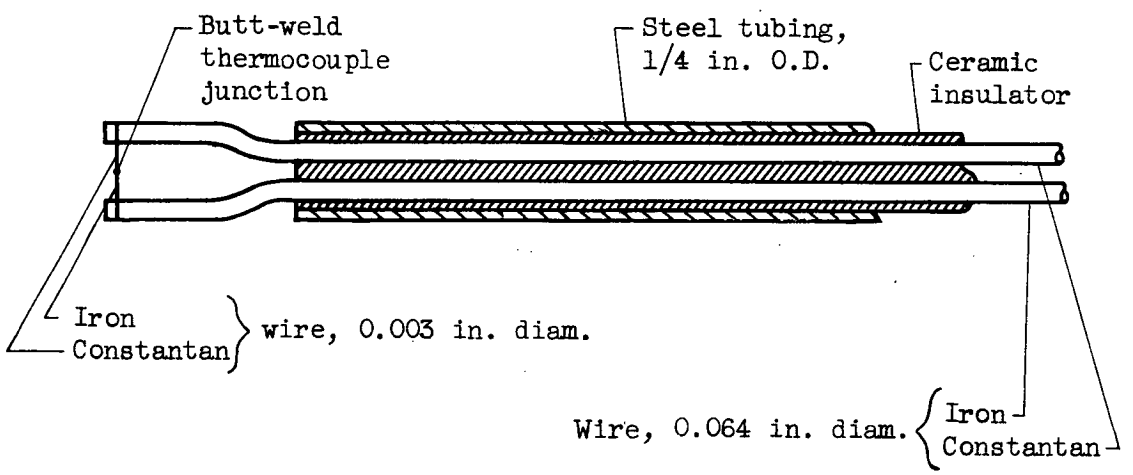

(b) Iron-constantan thermocouple.

Figure 3. - Measuring probes for air-temperature survey.

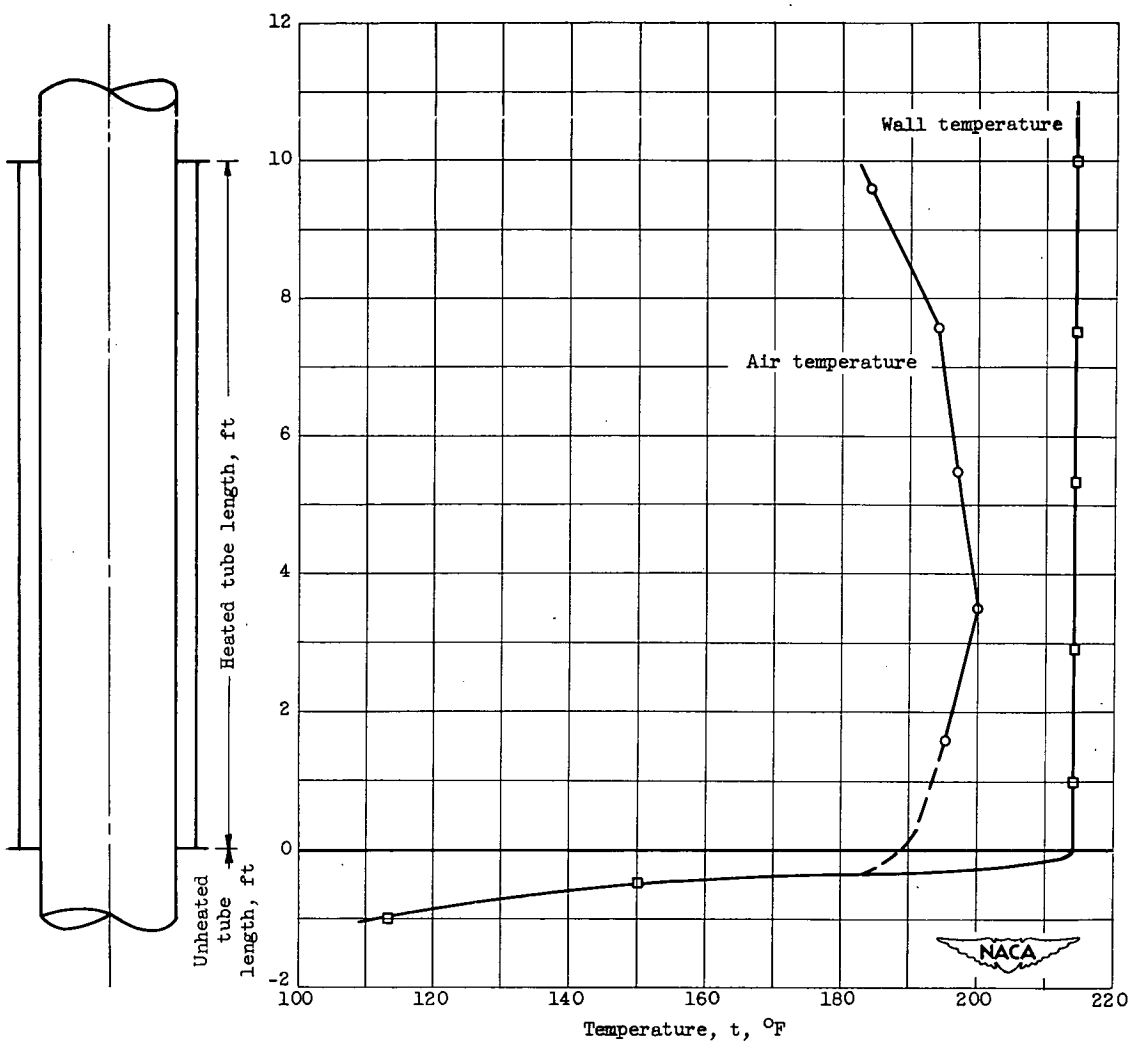

Figure 4. - Typical air-temperature distribution along tube axis and wall in heat-loss run.

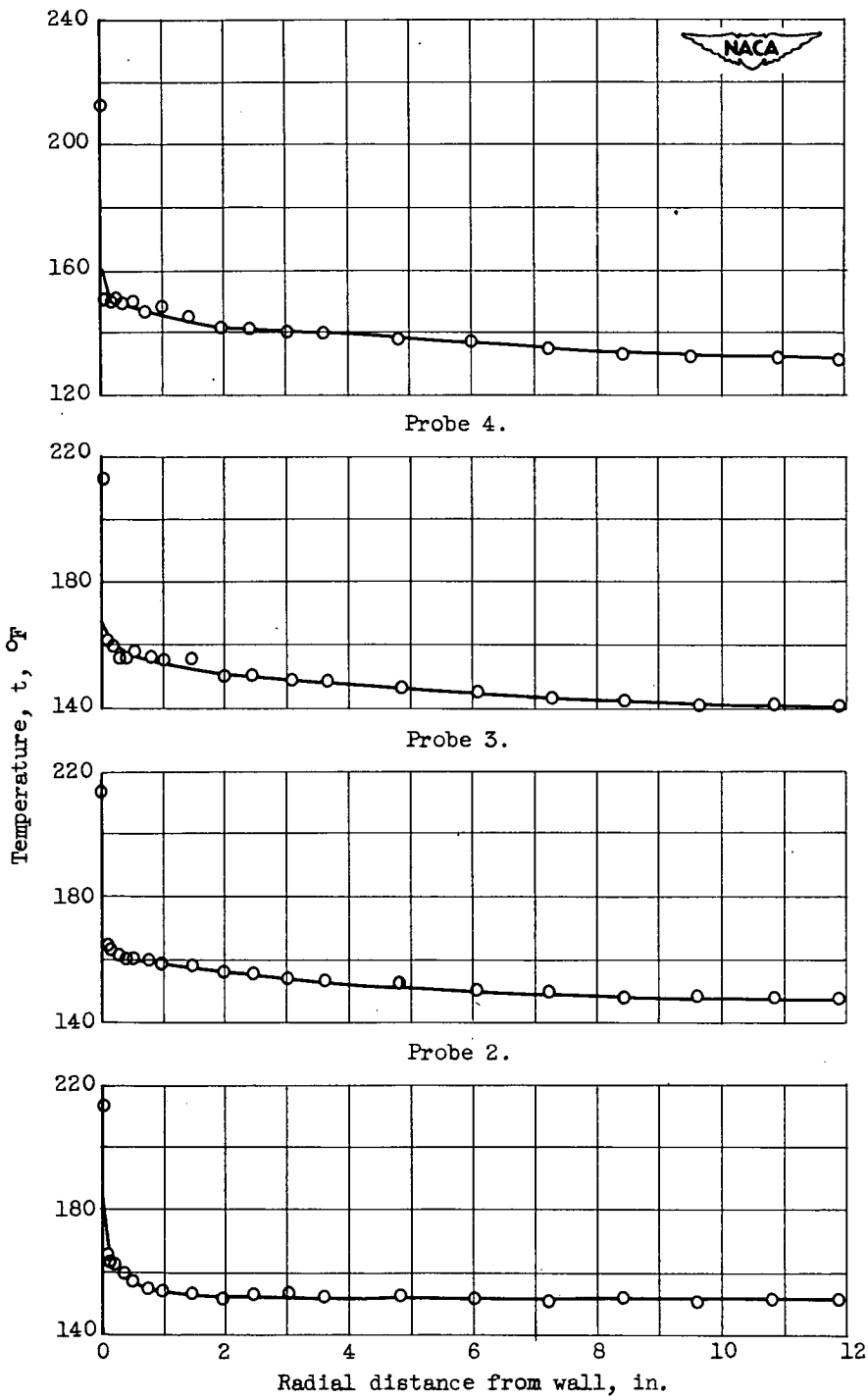

Figure 5. - Radial air-temperature profiles at four probe locations along axis for first cover configuration. Air pressure, 85 pounds per square inch absolute; air flow, 0.250 pounds per second.

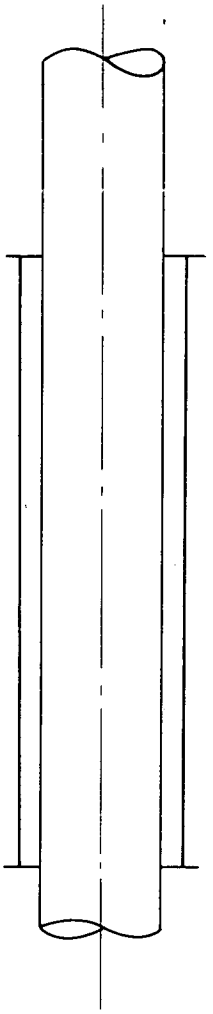

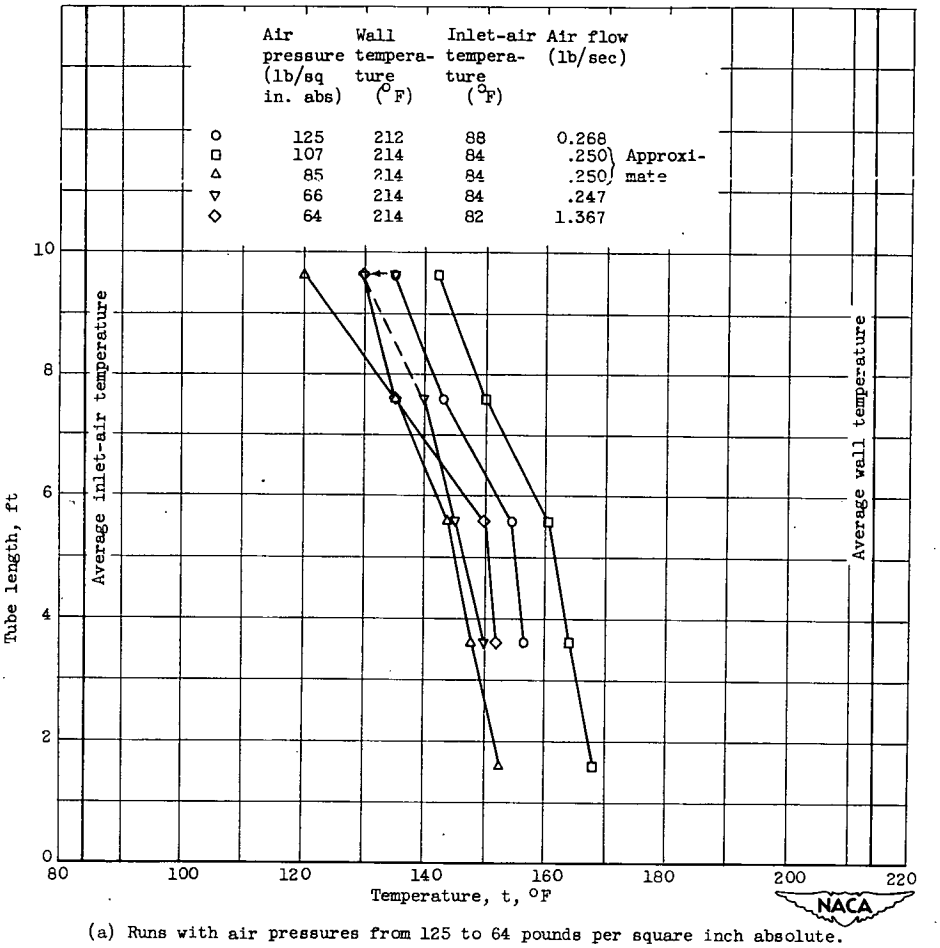

(a) Runs with air pressures from 125 to 64 pounds per square inch absolute.

Figure 6. - Temperatures of inlet air, air along tube axis, and wall for first cover configuration.

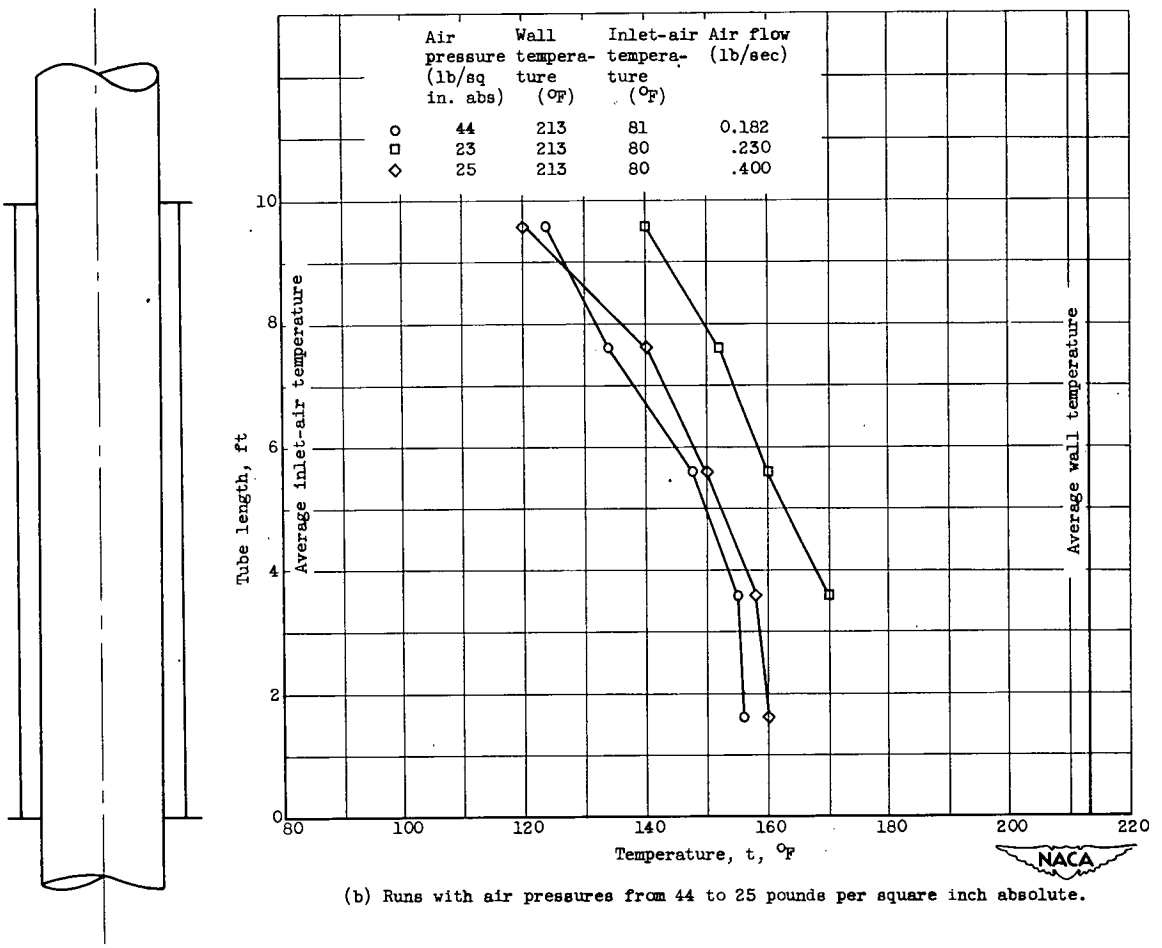

(b) Runs with air pressures from 44 to 25 pounds per square inch absolute.

Figure 6. - Concluded. Temperatures of inlet air, air along tube axis, and wall for first cover configuration.

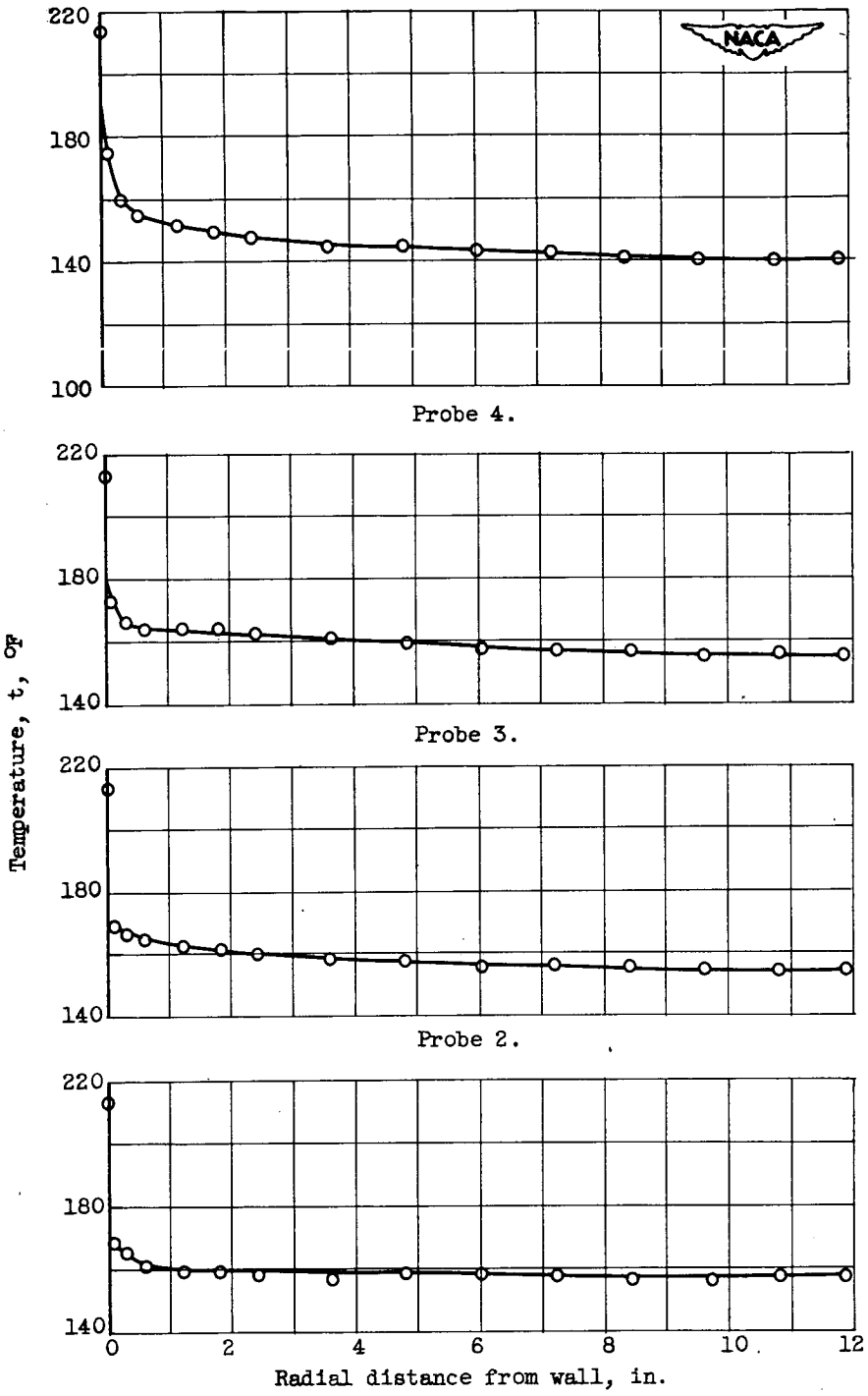

Figure 7. - Radial air-temperature profiles at four probe locations along axis for second cover configuration. Air pressure, 99 pounds per square inch absolute; air flow, 0.508 pounds per second.

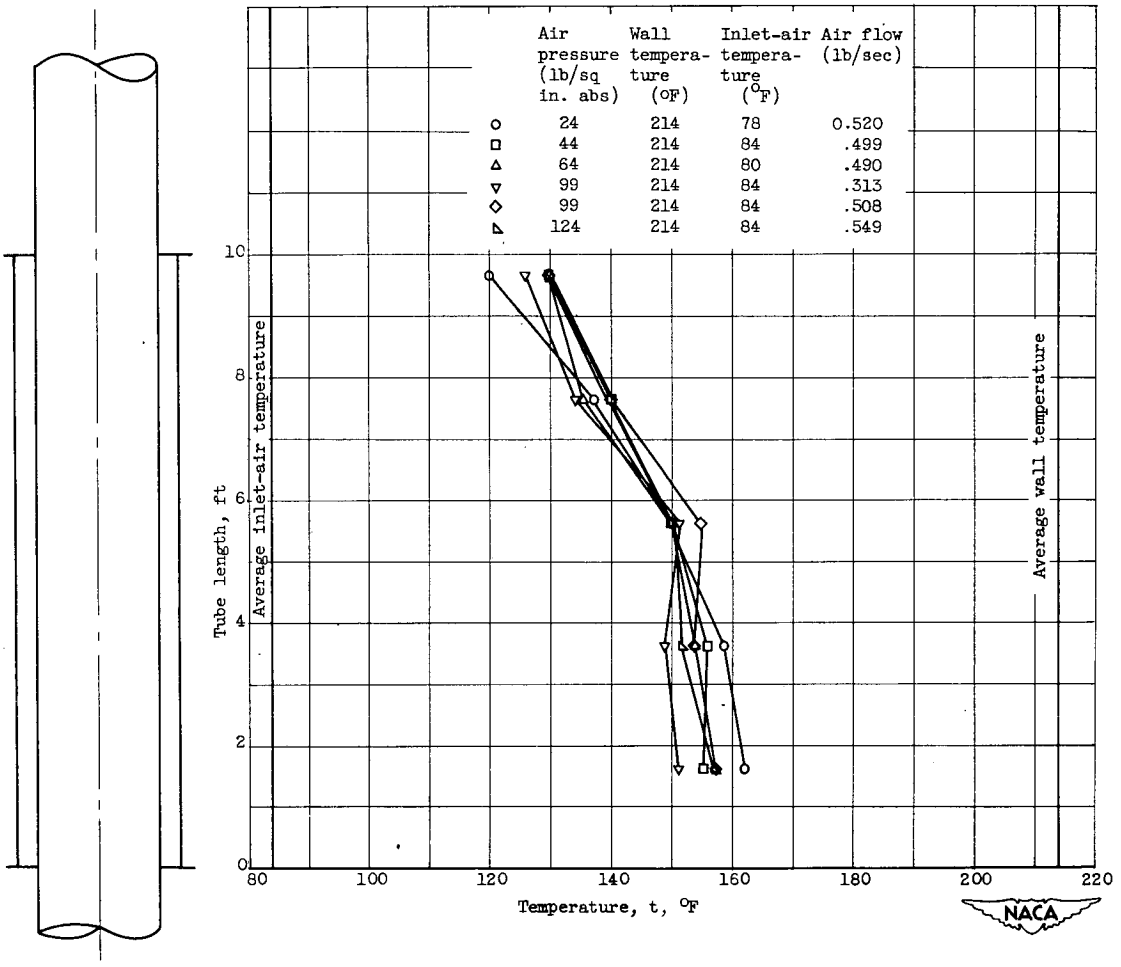

Figure 8. - Temperatures of inlet air, air along tube axis, and wall for second cover configuration.

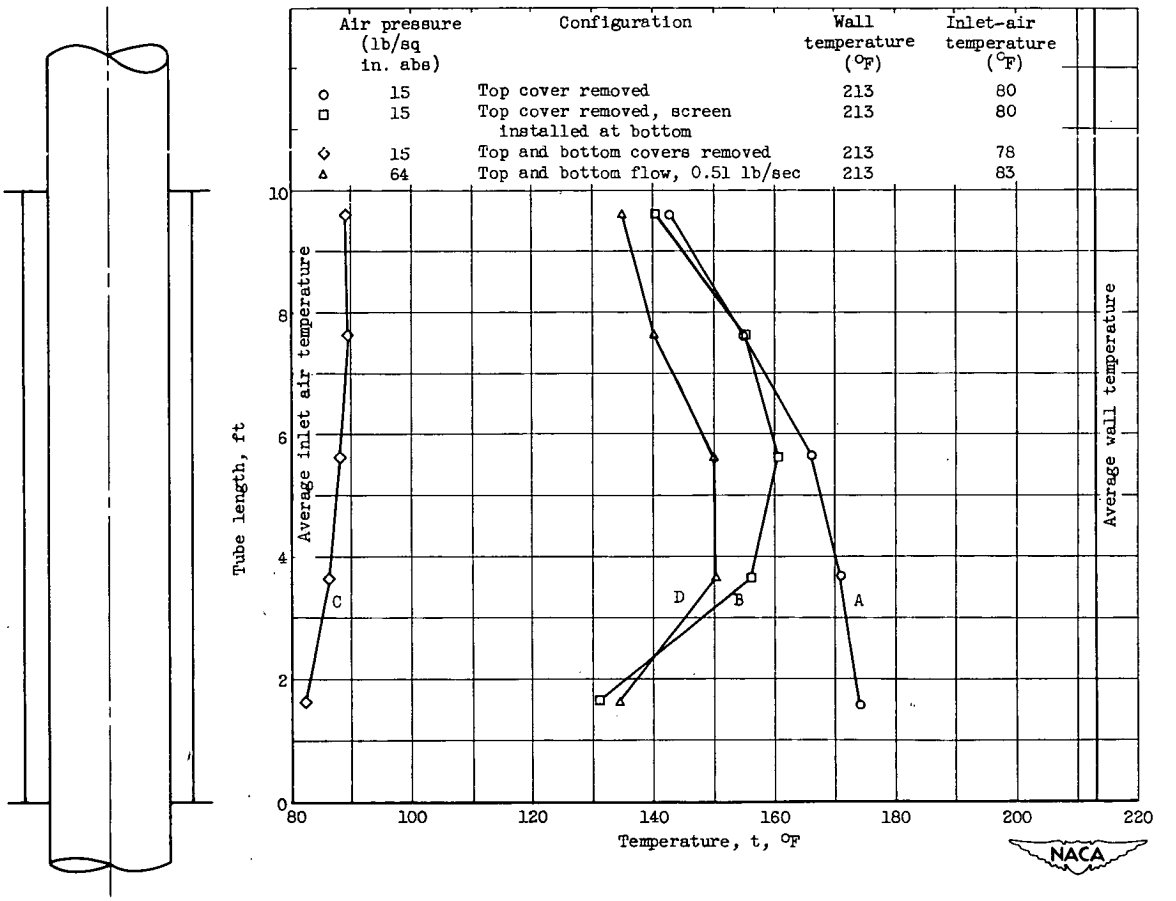

Figure 9. - Temperatures of inlet air, air along tube axis, and wall for various cover configurations.

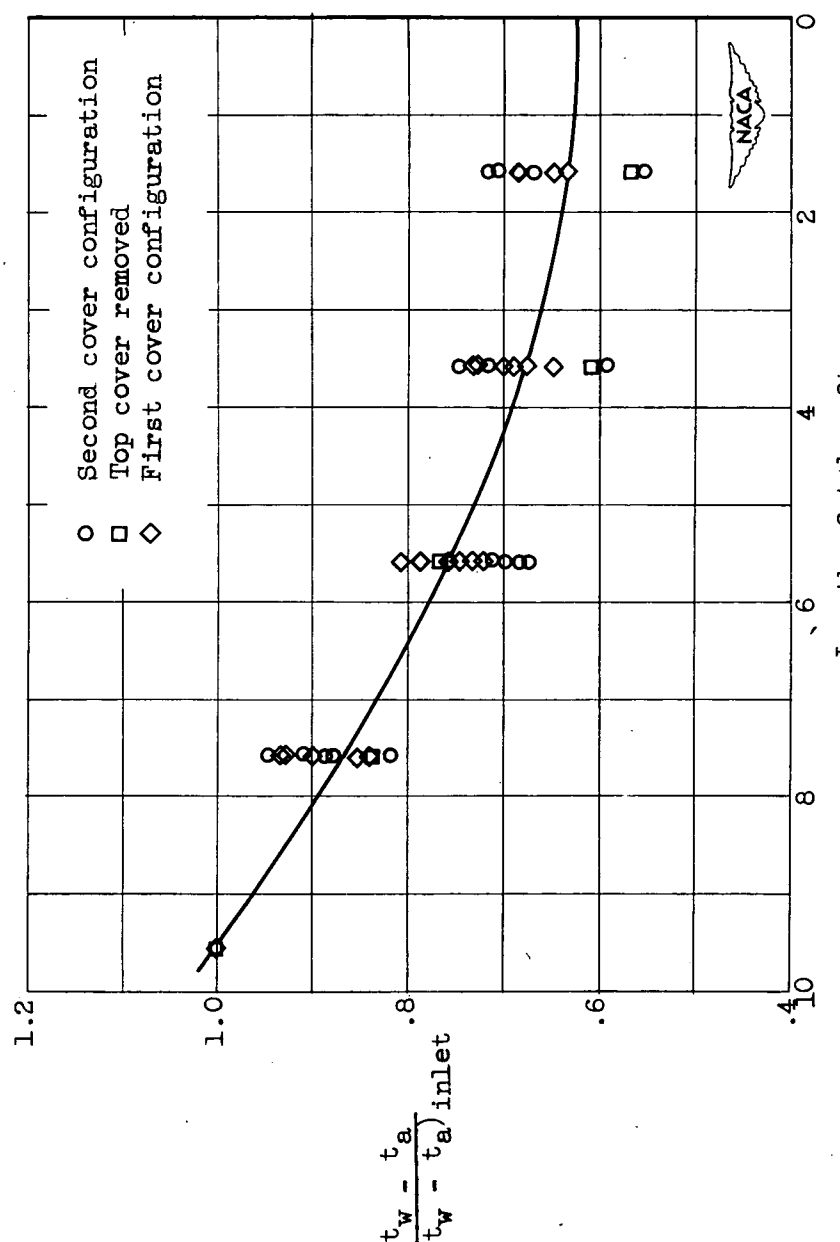

Figure 10. - Ratio of temperature differences along tube length between wall and air at center line to same temperature difference near inlet.

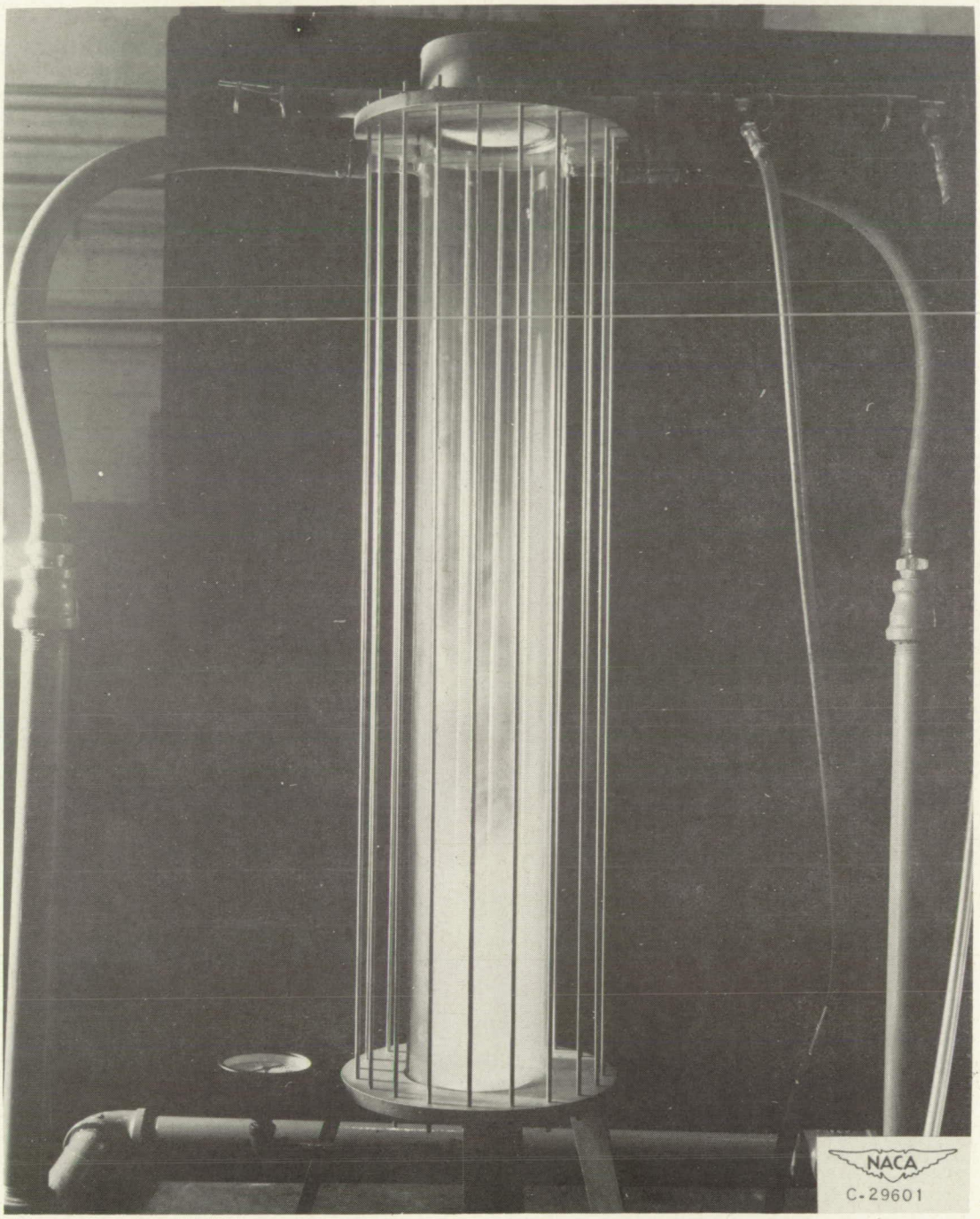

Figure 11. - Smoke test of flow inside glass scale model of tube indicating penetration of incoming air by decrease in smoke intensity.

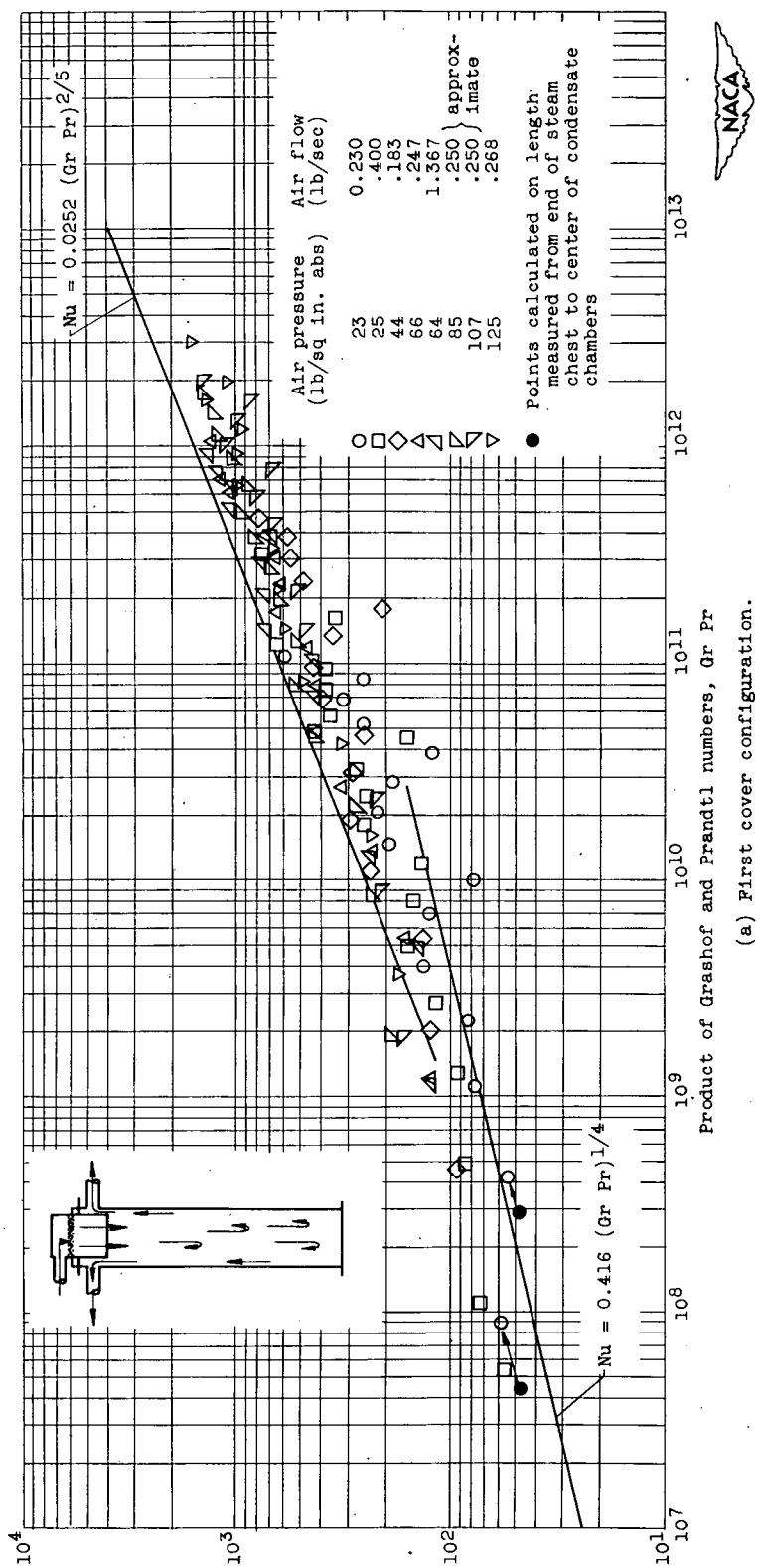

(a) First cover configuration.

Figure 12. - Dimensionless correlation of local free-convection heat-transfer coefficients in closed tube and comparison with known equations for vertical flat plate.

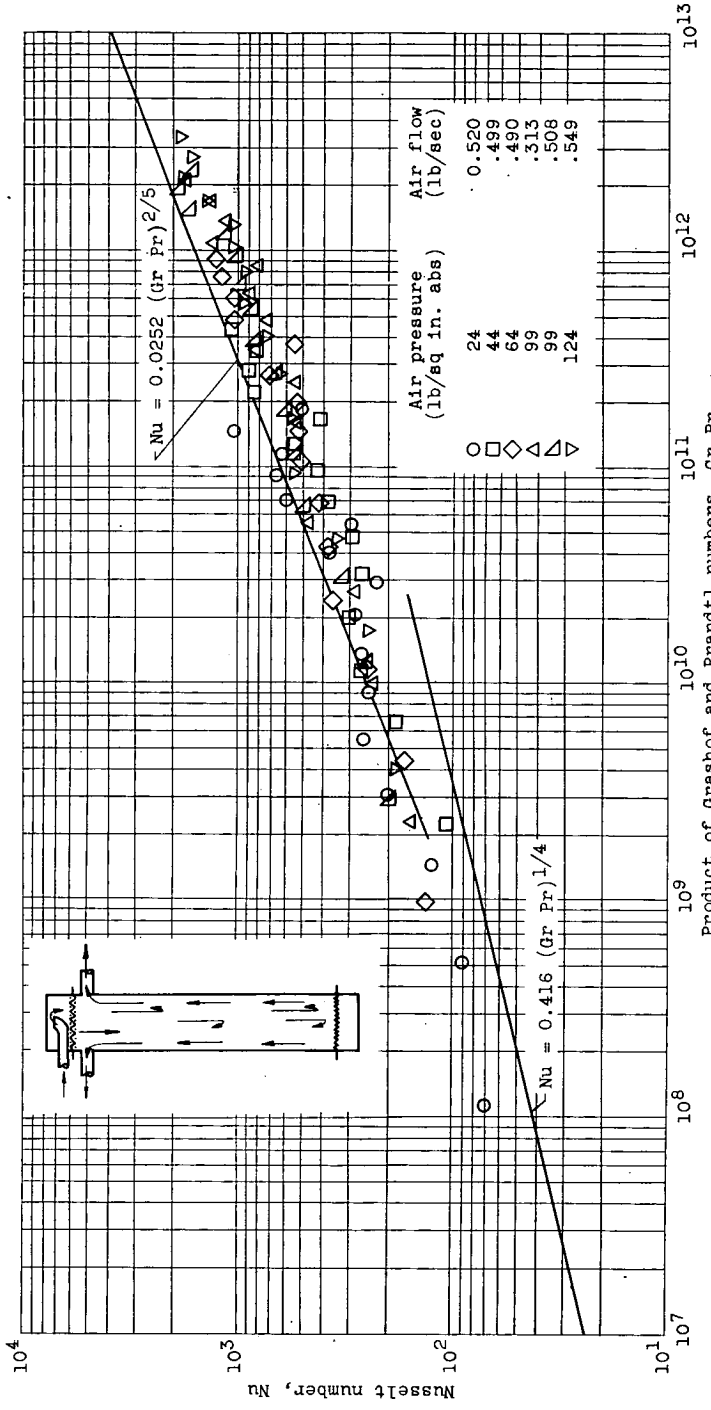

(b) Second cover configuration.

Figure 12. - Continued. Dimensionless correlation of local free-convection heat-transfer coefficients in closed tube and comparison with known equations for vertical flat plate.

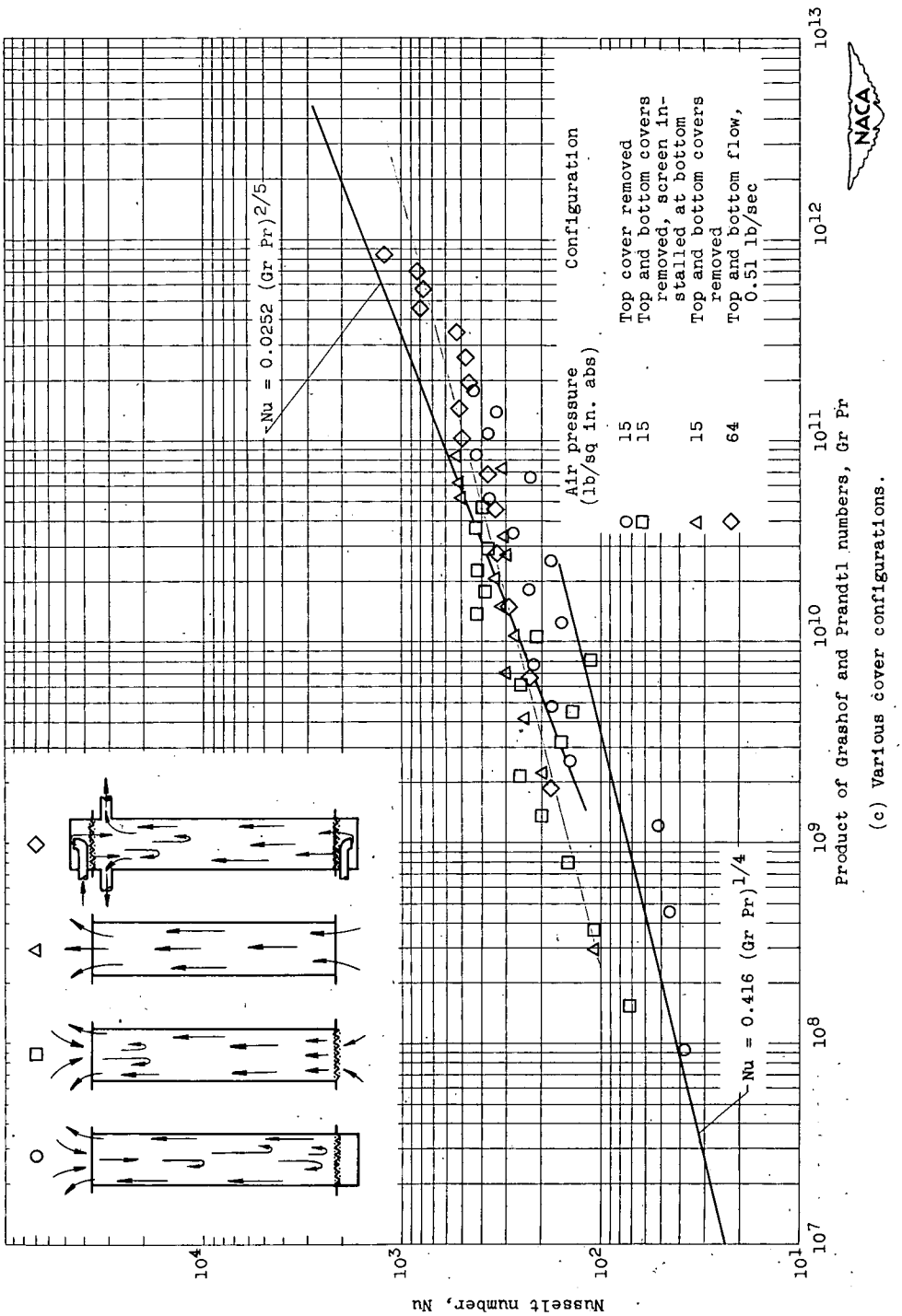

(c) Various cover configurations.

Figure 12. - Concluded. Dimensionless correlation of local free-convection heat-transfer coefficients in closed tube and comparison with known equations for vertical flat plate.

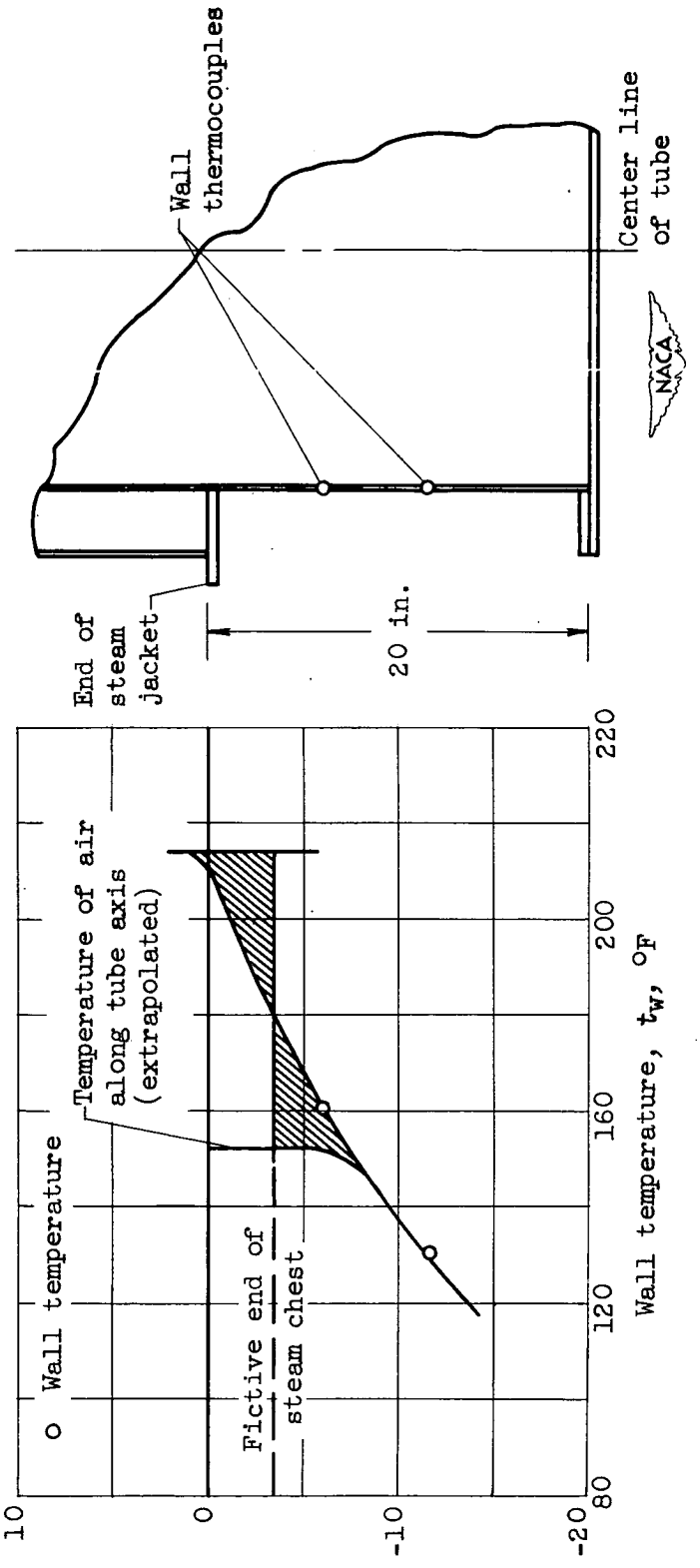

Figure 13. - Determination of fictive lower end of steam chest for comparison of local heat-transfer data with flat plate values.